



## DETERMINATION OF THE CONFINING EFFECT OF GEOGRID REINFORCEMENT FROM LARGE SCALE TRIAXIAL TESTS

Ho Van Thang

College of Engineering Technology, Can Tho University, Vietnam

---

### Article info.

Received date: 30/09/2015

Accepted date: 30/11/2016

---

### Keywords

Confining pressure, large-scale triaxial, geogrid reinforcement, peak strength, stiffness

---

### ABSTRACT

*The immense contribution of geogrids to the strength of reinforced soil is well known in science and nowadays also increasingly accepted in the industry. Reinforced granular material is a composite material which combines properties resistance of two different materials in such a way to increase its bearing capacity. However, the differences between calculated and measured deformations of geogrid-reinforced structures indicate that the exact behaviour of geogrids in soil is not totally understood yet. To allow for better assessment of the composite behavior, a series of large-scale triaxial tests were conducted on unreinforced and reinforced gravel specimens of 50 cm in height and 23 cm times 23 cm in cross-section, using an apparatus developed at the Institute of Industrial Science, University of Tokyo (Dan et al., 2006). In addition to the variation of the cell pressure, the test series also includes the variation of geogrid types.*

*Results of unreinforced and reinforced test series showed a significant increase of the peak strength as well as a reduction of the deformations of the tested samples due to the reinforcement. A confining effect of the reinforcement was clearly identified and could be explained with a mechanical model. A calculation method, which is based on the mechanical model, was used to draw the stress paths for a series of reinforced tests.*

---

Cited as: Thang, H.V., 2016. Determination of the confining effect of geogrid reinforcement from large scale triaxial tests. Can Tho University Journal of Science. Vol 4: 6-12.

### 1 APPARATUS, MATERIAL AND TEST PROCEDURE

The purpose of this study is to examine the effect of geogrids on the peak strength and the small strain stiffness of large prismatic specimen of gravel by conducting monotonic and large cyclic loading triaxial compression tests. A set of local deformation transducers (LDTs, Goto et al., 1991) and proximity transducers are used to measure strains

to minimize the effects of specimen corners, bedding error and system compliance. A large-scale triaxial apparatus (Dan et al., 2006) was employed to conduct triaxial compression tests on compacted gravel specimen. The large-scale triaxial apparatus and its stress control system are shown in Figure 1 and 2, respectively. The apparatus consists of triaxial cell, axial and lateral loading device, and a cell-pressure-control device. The axial loading device employs an electro-hydraulic actuator having a capacity of 490 kN and the zero balance system.

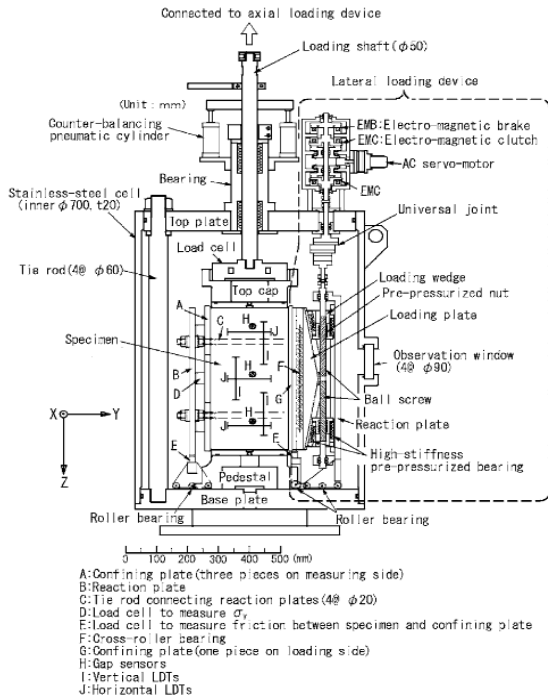


**Fig. 1: Large-scale triaxial apparatus**

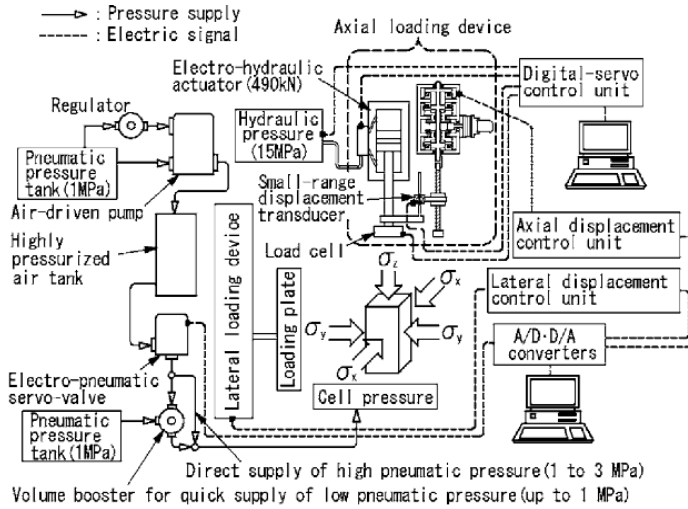


**Fig. 2: Stress control system of the large-scale triaxial apparatus**

For unreinforced tests, axial strain ( $\epsilon_1$ ) was measured by three pairs of vertical local deformation transducers (V-LDTs). Lateral strains in two directions ( $\epsilon_3$ ) were measured by another three pairs of horizontal local deformation transducers (H-LDTs). For in the reinforced tests, axial strain ( $\epsilon_1$ ) and lateral strains ( $\epsilon_3$ ) were measured by four pairs of vertical and horizontal local deformation transducers in each side of the specimen, respectively. The schematic diagrams showing the location of all LDTs over the specimen for both types of tests are shown in Figure 3. The mean of data measured with three or four pairs LDTs was used for each direction of local strain measurement for the analysis of test results.

The testing material was a well-graded crushed stone, called Tochigi gravel (Fig. 4). It consists of angular to sub-angular particles with a coefficient of uniformity  $C_u=32$  and specific gravity  $G_s=2.68$ . The optimum moisture content and the maximum dry density were defined by modified Proctor as  $w_{opt}=4.0\%$  and  $\rho_d=2.168 \text{ g/cm}^3$ , respectively.

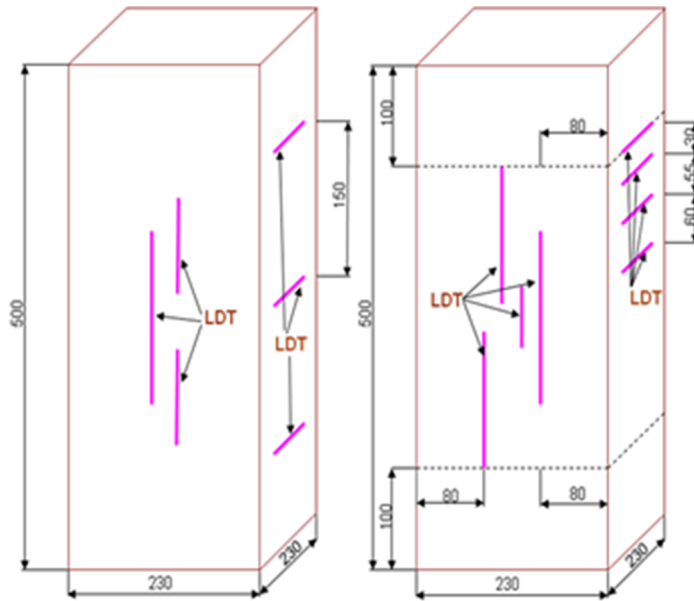


Fig. 3: Positioning of LDTs in case of unreinforced and reinforced tests

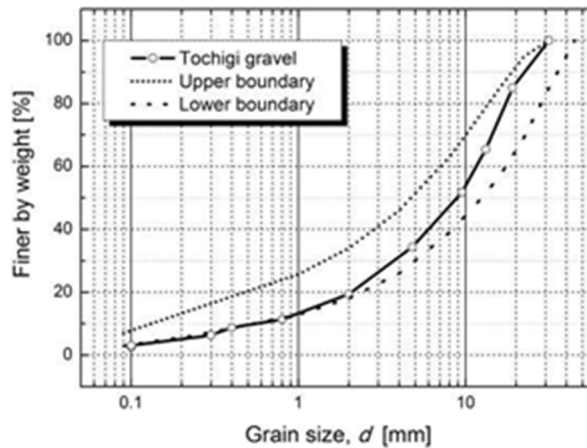


Fig. 4: Gradation curve of tested Tochigi gravel

The specimens were prepared by manual compaction at nearly optimum moisture content (Table 1). Specimens were compacted in 10 layers with a thickness of 5 cm for each layer. Before placing the material for the next layer, the surface of the previously compacted layer was scrapped to a depth of about 2 cm to ensure a good interlocking between vertically adjacent layers. The compaction was applied with an aim to reach dry density of specimen as close as possible to the one defined by Proctor test. In reality approximately 95% of the maximum density was reached on average. The confining pressure ( $\sigma_3$ ) was applied by vacuum

and by positive cell pressure and kept constant during testing. Two geogrid layers have been placed in the reinforced specimens leading to a vertical reinforcement spacing of nearly 0.3 m. Test results presented in this paper are obtained from specimen reinforced with a biaxial polypropylene (PP) and biaxial combi-polypropylene (Combi) geogrids with a nominal strength of 40 kN/m and welded, pre-stretched flat bars. The aperture size of the grid was 31mm x 31mm and the tensile force at 2% strain 16 kN/m, as given by the manufacturer. They can be shown in Figure 5.

**Table 1: Test conditions**

Test name	Reinforcement	$\sigma'_3$ (kPa)	$\gamma_d$	e	$\omega$ (%)
IIS-0E	Unreinf	25	2.053	0.31	3.73
IIS-0G	Unreinf	150	2,096	0.28	2.41
IIS-2D	Geogrid	150	2.089	0.28	3.81
IIS-2E	Geogrid	25	2.066	0.30	2.53
IIS-COM-C	Combi-grid	25	2.112	0.27	2.25
IIS-COM-D	Combi-grid	150	2.080	0.29	2.11

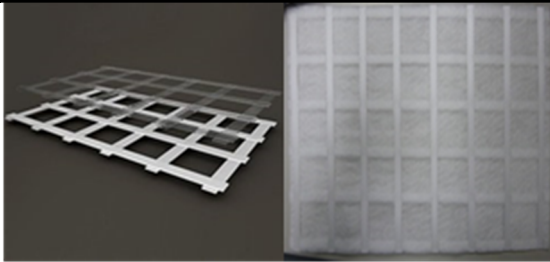


**Fig. 5: Figure of PP geogrid and Combi-PP geogrid, respectively**

**2 TEST RESULTS**

Stress-strain relationship of tests with unreinforced and reinforced samples compacted to 95% proctor density are given in Figure 6 for two types of geogrids at two different confining pressures of 25kPa and 150kPa. The increase of the peak strength due to the reinforcements can be seen clearly. The tests using PP geogrid show the highest peak strength in both low and high confining pressures.

However, the initial stiffness of both, unreinforced and reinforced specimens seems to be similar to each other for vertical strains up to about 0.3%. This is in accordance with the volumetric strains calculated from the radial and vertical strains, indicating almost pure compaction at the beginning of the tests (Fig. 7).

The reinforced test experienced negative dilatancy at larger axial strain than the unreinforced test. The unreinforced specimens initially contracted during unloading-reloading stage and started dilating at axial strains of about 0.3%. At the beginning of shearing stage, the unreinforced test almost reached the positive dilatancy side. During that, as shown in Figure 8, the PP geogrid did not show any dilatative behavior at confining pressure of 150 kPa. This is consistent with the above description regarding in Figure 6. In addition, Figure 8 shows that even at very low confining pressure of 25 kPa, the reinforced test using PP geogrid started dilating at vertical strain as nearly as the vertical strain at which the unreinforced test at 150 kPa started dilating. The geogrid can increase the peak strength of

the specimen without making the specimen expand laterally during its mobilization. That means the geogrid can increase the stiffness of the specimen.

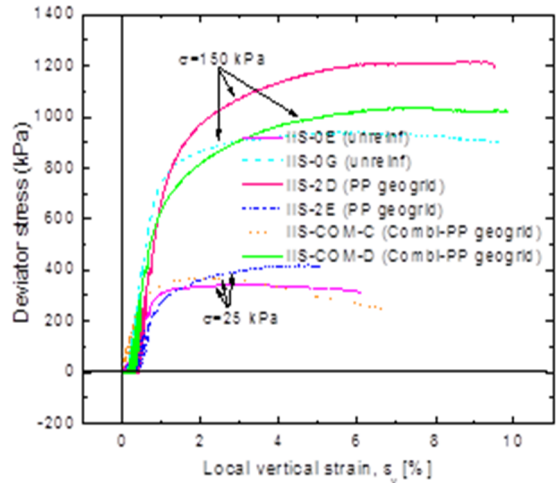


**Fig. 6: Stress-strain relationship**

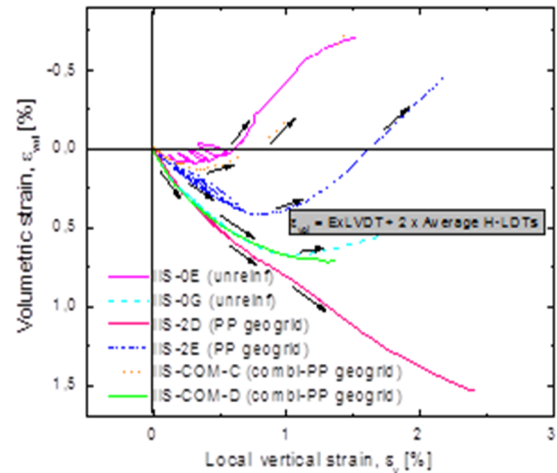


**Fig. 7: Volumetric strain of unreinforced and reinforced tests**

The development of reinforcement strains  $\epsilon_{reinf}$  with increasing vertical compression of the specimen is given in Figure 9. It is plotted for the strains measured at the center of the cross section, i.e. the maximum reinforcement strain.

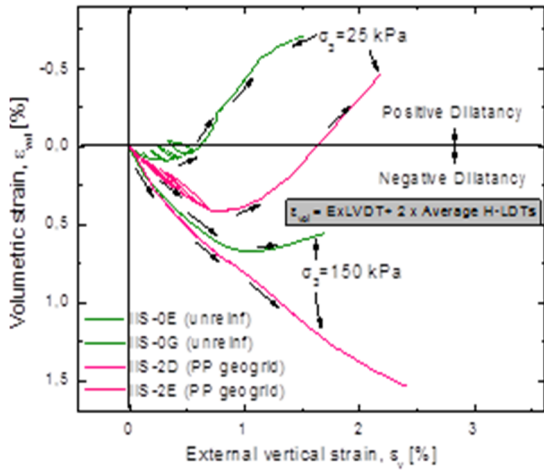


**Fig. 8: Volumetric strain of unreinforced and reinforced tests at 25 and 150 kPa**

The mechanical model shown in Figure 10 has been derived from the large triaxial testing results of the reinforced gravel. Caused by the vertical compression during loading the specimen extends radially. As stated above, this is accompanied by the activation of the geogrids, due to which the deformations are reduced and the peak strength is increased.

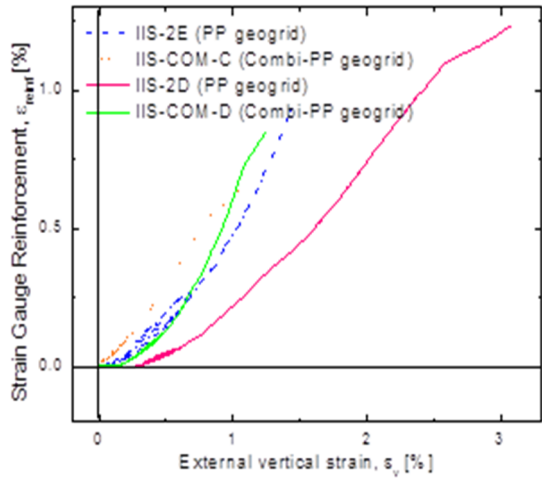


**Fig. 9: Strains distribution in the geogrids**

With progressive deformation of the specimen, the confining forces of the geogrids increased. As a simplified assumption, this can be considered as an equivalent, additional confining pressure  $\Delta\sigma_3$  acting homogeneously over the whole height of the specimen (Fig. 10), provided that the vertical spacing between the reinforcement layers are small enough.

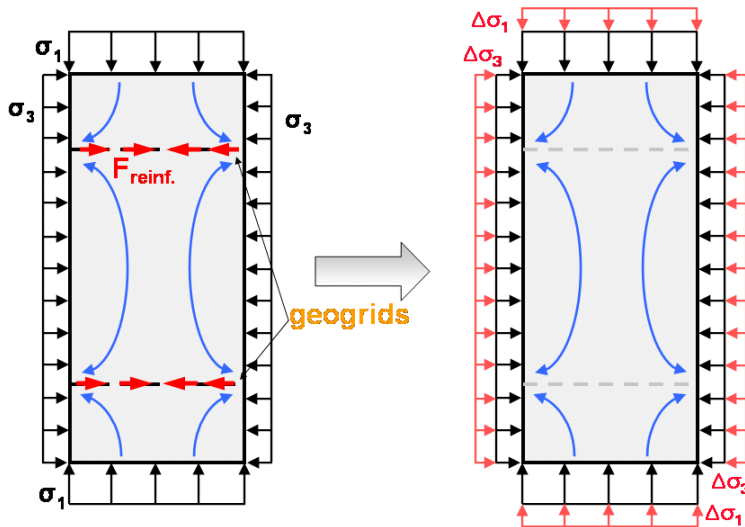


**Fig. 10: Increase of specimen strength due to reinforcement**

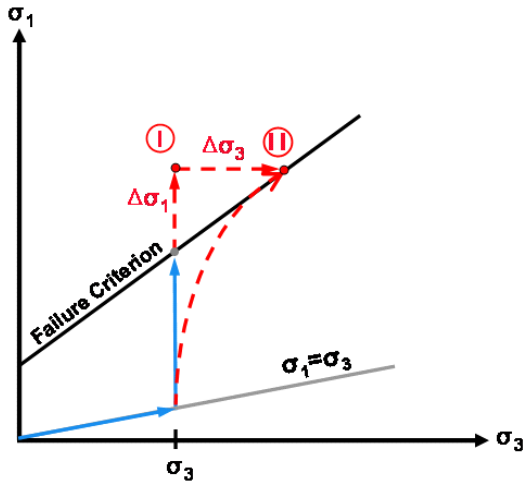


**Fig. 11: Stress path of the loading due to reinforcement**

In Figure 11 stress paths of an unreinforced and a reinforced specimen are drawn qualitatively. The scale of the axis in the diagram is different from usual in order to show up the details. Therefore, the straight line  $\sigma_1 = \sigma_3$ , which would normally be the bisecting line is less inclined. In both tests the specimens are being consolidated under isotropic conditions before loading. The stress path in unreinforced test (case I) shows an increase of  $\sigma_1$  until

failure while the confining pressure  $\sigma_3$  is kept constant. In a reinforced test (case II), an increase of  $\sigma_1$  beyond the critical limit of the unreinforced tests can be observed, although the confining pressure is the same as it was for the unreinforced test. The stress condition results at failure for “case I” is therefore  $\{\sigma_1 + \Delta\sigma_1; \sigma_{3,cell}\}$ . However, due to the deformation under activation of the geogrids and according to the model described above, the stress condition for case II will be affected by an increase of the confining pressure by  $\Delta\sigma_{3,ref}$  during loading. When failure eventually occurs, the stress condition reaches the failure criterion of the unreinforced soil (case I), but at a much higher stress level  $\{\sigma_1 + \Delta\sigma_1; \sigma_{3,cell} + \Delta\sigma_{3,ref}\}$ .

The stiffness of the specimens derived from small cyclic loading is shown in Figure 12. As can be seen, the reinforcement does not largely affect to the small strain stiffness of the specimens under either low or high confining pressures.

Figure 13 shows that deformations of reinforced specimens are less than those of unreinforced specimens at low confining pressures. At high confining pressures, on the other hand, there was almost no effect of reinforcement.

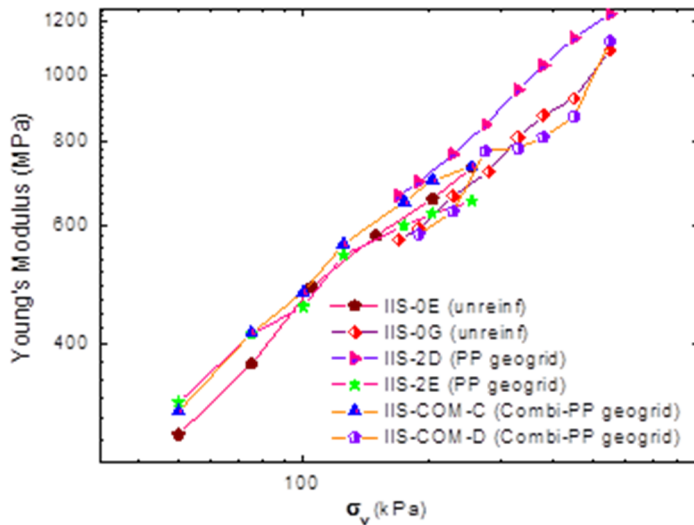


**Fig. 12: Stiffness of unreinforced and reinforced specimens**

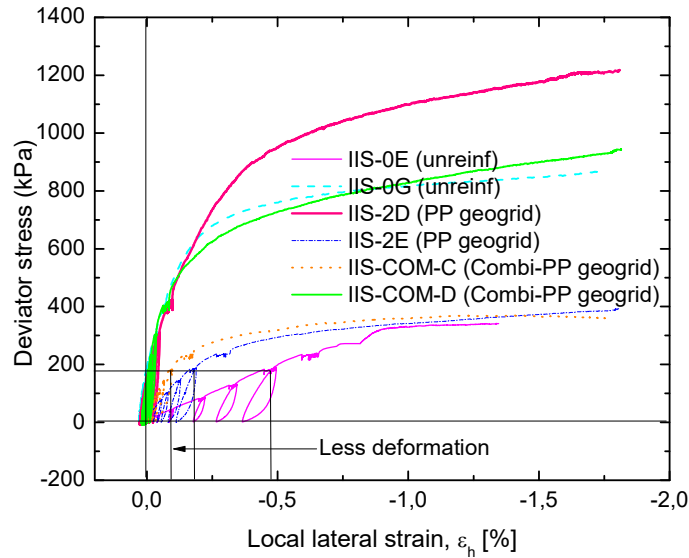


**Fig. 13: Reduction of deformations due to mobilization of reinforcement**

### 3 CONCLUSIONS

Large-scale triaxial tests on reinforced and unreinforced specimens showed a significant increase of the peak strength and reduction of the deformations due to the geogrids. The result is consistent with observations made in field. Geogrid reinforced soils develop an additional confining effect due to activation of the geogrids. The relative reinforcing effect is higher for small lateral confining pressures, at small depths.

Geogrid reinforcement does not show any significant improvement in the small strain stiffness of granular. The tests using PP geogrid have a higher performance than the tests using combi-grid in case of using gravelly soil. Therefore there should be a consideration in using the correct type of geogrids corresponding to the construction materials.

### REFERENCES

Dan, L.Q.A., Koseki, J., Sato, T., 2002. Comparison of Young's Moduli of dense sand and gravel measured by dynamic and static methods. *Geotechnical Testing Journal*, ASTM. 25(4): 349-368.

Abu-Hejleh, N., Zornberg, J.G., Wang, T., Watcharamonthein, J., 2002. Monitored displacement

of unique geosynthetic-reinforced bridge abutments. *Geosynthetics International*. 9(1): 71-95.

Moghaddas-Nejad, F., Small, J.C., 2003. Resilient and permanent characteristics of reinforced granular materials by repeated load triaxial tests, *Geotechnical Testing Journal*, ASTM. 26(2): 152-166.

Ziegler, M., Timmers, V., 2004. A new approach to design geogrid reinforcement, *Proceedings of Euro-Geo3*, DGGT, Munich, Germany. 2: 661-666.

Dan, L.Q.A., Koseki, J., Sato, T., 2006. Evaluation of quasi-elastic properties of gravel using a large-scale true triaxial apparatus, *Geotechnical Testing Journal*, ASTM. 29(5): 374-384.

Ruiken, A., Ziegler, M., 2008. Effect of Reinforcement on The Load Bearing Capacity of Geosynthetic Reinforced Soil, *EuroGeo4*, IGS, Edinburgh, UK.

Maqbool, S., Koseki, J., 2010. Large-Scale Triaxial Tests to Study Effect of Compaction Energy and Large Cyclic Loading History on Shear Behavior of Gravel, *Soils and Foundations*. 50(5): 633-644.

Lenart, S., Koseki, J., Sato, T., Miyashita, Y., Ho, V.T., 2012. Large-scale triaxial tests of dense gravel material at low confining pressure, *Advances in Transportation Geotechnics*, Hokkaido International Conference: 587-592.

Ho, V.T., 2012. Mechanical Characteristics of Geogrid-reinforced Gravel in Large-scale Triaxial Tests. Master thesis. The University of Tokyo, Japan.